Polymer Degradation and Stability 144 (2017) 344–353

Contents lists available at ScienceDirect

Polymer Degradation and Stability

journal homepage: www.elsevier.com/locate/polydegstab

Modeling the ignition of poly(methyl methacrylate)/carbon nanotube nanocomposites

A. Galgano [a], C. Branca [a], C. Di Blasi [b, c, *], P. Vollaro [c], E. Milella [c]

[a] Istituto di Ricerche sulla Combustione, C.N.R., P.le V. Tecchio, 80125 Napoli, Italy
[b] Dipartimento di Ingegneria Chimica, dei Materiali e della Produzione Industriale, Università degli Studi di Napoli "Federico II", P.le V. Tecchio, 80125 Napoli, Italy
[c] IMAST, Distretto Tecnologico sull'Ingegneria dei Materiali Polimerici e Compositi e Strutture P.zza Bovio, 22, 80133 Napoli, Italy

ARTICLE INFO

Article history:
Received 25 May 2017
Received in revised form
28 July 2017
Accepted 11 August 2017
Available online 14 August 2017

Keywords:
Nanocomposites
Ignition

ABSTRACT

A transient one-dimensional model, including the description of the chief chemical and physical mechanisms of the thermo-oxidative decomposition of poly(methyl methacrylate)/carbon nanotube composite and the parent polymer, combined with the critical mass flux criterion, quantitatively predicts the ignition times measured in a cone calorimeter. At low heat fluxes, the ignition times are longer for the composite, owing to the flame retardancy action of the carbon nanotubes resulting in the formation of a surface charred barrier, prior the attainment of sufficiently high rates of volatile release. Instead, at high heat fluxes, surface (versus in depth) absorption of the thermal radiation locally enhances the decomposition rate leading to shorter ignition times for the composite. Of paramount importance for the quantitative prediction of the ignition time is not only the empirical criterion (critical surface temperature or volatile mass flux) but also accurate kinetics taking into account the polymer properties, in particular the polymerization degree, and the presence of oxygen during the initial transient stage.

1. Introduction

The dispersion of nanoparticles of different nature within a polymeric matrix leads to improved fire retardancy performances of composite materials [1–4]. The analysis of a huge amount of experimental data, also with the aid of mathematical modeling [5–10], demonstrates that the formation of a thermally insulating layer at the heat-exposed surface of the specimen highly protects the virgin material underneath, in this way delaying the devolatilization reactions. It is possible that the formation of a charred superficial layer also affects the mass transfer processes, such as the escape of bubbles in the polymer melt [8].

In accordance with the data produced from cone calorimetry tests [11], flame retardancy of polymer nanocomposites usually causes a drastic reduction in the peak of the heat release rate and the average mass loss rate. However these positive features are associated with a rather low impact on the ignitability [12,13], often with a reduction in the ignition times (see, for instance [14–22]). Different explanations have been given for this undesired result which include modifications in the medium thermal properties (surface absorption and/or effective thermal conductivity) [17,19,23,24] or thermal degradation of the additive [15,25] and modifications in the thermal degradation pathways [22,26–29]. Although the mechanism responsible for the acceleration in the ignition of nanocomposites can be material specific, it is evident that there is not sufficient experimental data to reach a consensus about this issue. Moreover, from the theoretical point of view, only a qualitative analysis, essentially using the heat conduction equation for thermoplastic polyurethane and polyamide-6 [23], is available. It is speculated that the effective thermal conductivity of the nanocomposite and the parent polymer are functions of the temperature. Though at low temperatures the nanocomposite exhibits higher thermal conductivity subsequently, due to the changes in the rheological behavior, that of the polymer becomes higher. Thus, given the same ignition temperature, the nanocomposite ignites first. However, it is understandable that, given the highly simplified model, this conclusion cannot be considered of general validity and further investigation is also needed from the theoretical side.

Detailed modeling of the solid phase processes of nanocomposites and the parent polymer could indeed represent a

* Corresponding author.
E-mail address: diblasi@unina.it (C. Di Blasi).

http://dx.doi.org/10.1016/j.polymdegradstab.2017.08.013
0141-3910/

powerful tool to ascertain the mechanisms responsible for flame retardancy as shown by the comprehensive solid-phase model [9,10] recently developed for the degradation of thermoplastic polymer/carbon nanotube composites and the parent polymers. The model was experimentally validated against temporal profiles of the mass loss rates for a configuration mimicking cone calorimeter heating under an inert environment and exploited to understand the role of the chemical and physical processes. By coupling with an adequate empirical criterion, the transport model can also be extended to simulate nanocomposite ignition whose controlling mechanisms, as already pointed out above, are unknown. This approach is used in this study in combination with experimental investigation, stressing that none of the other comprehensive models available in the literature has ever been adapted/applied to investigate the ignitability properties of thermoplastic polymer nanocomposites.

In this study thermogravimetric curves are measured, at variable heating rates, of a high-molecular weight poly(methyl methacrylate) (PMMA) sample, for both inert and oxidative environment, and applied for the development of multi-step mechanisms including the estimation of the kinetic parameters. Then the comprehensive transport model of the degradation of poly(methyl methacrylate)/carbon nanotube (PMMA/CNTs) composites and PMMA, previously developed [9,10] but extended to include the multistep kinetics, is applied to predict the ignition times for the two materials using the criterion based on the attainment of either a critical surface temperature or a critical mass flux. Both criteria are examined owing to their possible influences on the determination of the controlling mechanism. Experimental validation is made using the measured ignition times in a cone calorimeter for irradiances in the range 15–75 kW/m^2. A parametric analysis (influences of the critical surface temperature/mass flux values, thermal versus thermo-oxidative decomposition, low- and high-molecular weight polymer) is also carried out. Finally the simulations are analyzed to shed light on the role of carbon nanotubes on PMMA ignition.

2. Experimental details

In order to carry out the experimental validation of the model, experimental activities have been undertaken for PMMA and the PMMA/CNTs nanocomposite. PMMA in powder (code M0088, CAS: 9011-14-7 Lot: QNS4G) was purchased from Tokyo Chemical Industries (TCI) CO. Ltd. Japan. Multi-wall carbon nanotubes (Nanocyl™ NC 7000, Nanocyl) were used as flame retardant fillers. Pure polymer and composite were processed on a twin counter rotating internal mixer connected to a control unit (Rheomix 600 and PolyLab QC, respectively, Haake, Germany). Before mixing, the materials were previously dried in vacuum oven for 24 h at 333 K. The temperature profile used during the extrusion was 493/513/503 K in the respective feeding/mixing/matrix zones with rotation of 45–50 rpm. The selected extrusion conditions were in the range of the optimal ones previously determined [30] by electron microscopy for the dispersion of CNTs into the PMMA matrix, minimizing the aggregate size. Good dispersion was generally achieved for CNTs loadings between 0.1 and 10 wt% with the best dispersions at the lower loading levels, such as that applied in this study. Moreover no nanotube damage (tube breakage or alterations in the surface morphology) was observed. The extruded materials were cooled in water and subsequently reduced to granules with the aid of a pellettizzator. Carbon nanotubes were added in the proportion of 1 wt% to PMMA. After extrusion, pure polymer and composite were compression molded at 513 K and 50 bar into 15 mm-thick slabs by a hot press (P300P, Collin, Germany).

Experiments were made, by means of a thermogravimetric system, for pure PMMA, aimed at the analysis of the thermal and thermo-oxidative kinetics, and a cone calorimeter for both pure PMMA and PMMA/CNTs slabs, focused at the evaluation of the ignition times. Thermogravimetric curves were measured using the commercial system Mettler TGA/1, with a pulverized sample mass of 5 mg heated under a flow of 50 ml/min, using heating rates of 2.5, 5 and 10 K/min up to 800 K, both in air and nitrogen. It was observed that a kinetic regime, required for the determination of intrinsic kinetics, is certainly established for heating rates below 15 K/min and sample mass up to 5 mg. In general, for this regime, it is necessary to measure weight loss curves in the absence of heat and mass transfer limitations, that is, the sample temperature must coincide with the heating temperature and the oxygen concentration (this only for thermo-oxidative kinetics) across the sample should be the same as the that at the sample surface (no spatial gradients and negligible differences between the sample conditions and those of the surrounding environment). From the practical point of view, such conditions are accomplished by lowering the heating rate and the sample mass (thickness) until no change is seen in the measured mass fraction and devolatilization rate curves. The DSC1 STAR system Mettler was used for the evaluation of the global decomposition heat using a sample mass of 5.5 mg heated at 10 K/min up to 800 K. The combustion tests were carried out by the Oxygen Consumption Calorimeter (Cone Calorimeter) following the ISO 5660 procedure (horizontal configuration). Specimens of 100 × 100 mm^2 and thickness of 15 mm were employed for cone irradiance levels of 15, 20, 25, 35, 50 and 75 kW/m^2. The ignition time was evaluated as in Hopkins (1995) [31], that is, as “the time at which a continuous flame is supported on the material surface”, independently from the appearance of prior flashing events.

3. Thermal and thermo-oxidative decomposition kinetics

The decomposition kinetics of PMMA depends on the polymerization process and the molecular weight/polymerization degree [32]. The reaction environment, either inert or oxidative, also affects the decomposition of polymeric materials [20]. The thermogravimetric curves measured for the PMMA sample (Fig. 1, heating rate 5 K/min) confirm the important role of oxidative versus thermal degradation with results that are in agreement with those reported in Ref. [33]. Oxygen increases the polymer stability at low temperatures and enhances random scission at high temperatures. In fact, compared with the inert atmosphere, the devolatilization rates are initially (temperatures below 500 K) lower but successively they become higher with the absolute peak rate

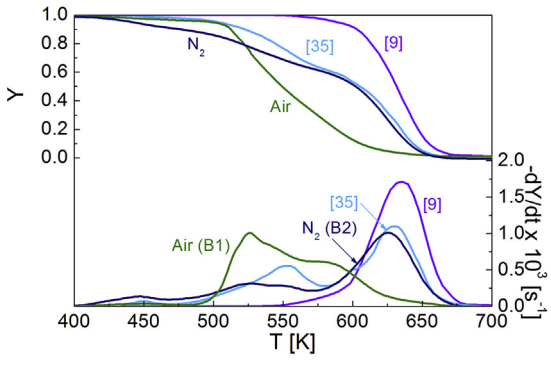

Fig. 1. Thermogravimetric curves for the mass fraction, Y, and mass loss rate, -dY/dt, versus temperature for the PMMA sample of this study in air and nitrogen and the PMMA samples discussed in the studies of Ref. [9] and Ref. [35] in nitrogen (heating rate 5 K/min).

positioned at about 525 K versus 626 K. Moreover quite complicated dynamics appear, representative of a multi-step devolatilization process, with peaks/shoulders again affected by the reaction environment.

It is worth recalling that PMMA decomposition has been extensively modeled by means of a single-step reaction. Examples are the kinetic evaluations reported in Ref. [9] for PMMA with a molecular weight of 100000 g/mol (the curves for a heating rate of 5 K/min are included in Fig. 1 for comparison) and Ref. [34]. The molecular weight of the PMMA sample of this study is not made available from the producer but it can be reasonably speculated that it is much higher, presumably by an order of magnitude, with respect to that of the single-step sample. Indeed, by way of example, Fig. 1 also reports the thermogravimetric curves, in nitrogen, for a PMMA sample with a molecular weight of 996,000 g/mol [35], showing a multi-step devolatilization process similar to that of the TCI sample of this study. Moreover, it is plausible that not only the molecular weight is approximately the same but also the polymer is obtained by free radical synthesis and thermal decomposition occurs according to the same mechanism reviewed in Ref. [35]. In particular, the first peak rate, around 425 K, is attributed [36] to the first reaction step initiated by radical transfer to unsaturated chain ends.

The intrusion of heat/mass transfer effects in thermogravimetric analysis is favored when the PMMA/CNTs sample is considered, owing to the possible formation of a surface barrier. In principle, this only modifies the heat/mass transfer rates and not the polymer decomposition kinetics, given that it acts through physical (not chemical) mechanisms to cause fire retardancy. However, though the conditions for the attainment of a chemical regime become more stringent, it has been found (for instance, Refs. [37,38]) that CNTs do not affect the thermal stability of the polymer. Therefore thermogravimetric curves have been measured only for pure PMMA and the related kinetic parameters are assumed to remain invariant for the corresponding composite.

The kinetic model proposed in this study is based on the evaluation of the thermogravimetric curves measured at different heating rates (2.5, 5 and 10 K/min). Following the approach extensively applied for the devolatilization of condensed-phase fuels [39–44], it is assumed that volatile fractions are released according to a set of parallel reactions for the lumped components. More specifically, a set of four parallel reactions gives good predictions of the thermogravimetric curves with parameters that depend on the reaction environment (kinetics B1 for oxidative degradation and kinetics B2 for thermal degradation). The reaction rates present an Arrhenius dependence on the temperature and a power-law dependence on the condensed-phase mass fraction. The component dynamics are described by four ordinary differential equations written for the mass fractions, Y_i, of the reacting polymer:

$$\frac{d}{dt}Y_i = -A_i \exp\left(-\frac{E_i}{RT}\right) Y_i^{n_i}; \quad Y_i(0) = \nu_i, \quad i = 1,2,3,4 \tag{1}$$

where the temperature, T, is a known function of time.

The kinetic parameters A_i (pre-exponential factors), E_i (activation energies), n_i (reaction orders), ν_i (stoichiometric coefficients, that is, the total mass fractions of volatiles released from each reaction step) are numerically estimated considering simultaneously both TG and DTG data for the various heating rates, following the method already described [39] and based on simultaneous nonlinear regression of the curves. The estimated parameters are practically invariant with the heating rate. Finally deviations between measurements and predictions, dev_{TG} and dev_{DTG}, are defined as in Ref. [39]. The estimated data are listed in Table 1 and examples of the component dynamics and a comparison between predictions and measurements can be made through Fig. 2 and Fig.3A–B, respectively.

Table 1
Parameters (activation energy, E, pre-exponential factor, A, reaction order, n, stoichiometric coefficient) for the four-step kinetic model developed to describe PMMA decomposition in air (mechanism B1) or nitrogen (mechanism B2) and deviations between measurements and predictions for the integral (%dev_{TG}) and differential (%dev_{DTG}) thermogravimetric curves.

Parameter	Air (B1)	N_2 (B2)
E_1 [kJ/mol]	118.0	
A_1 [s^{-1}]	1.3×10^{12}	
n_1	1.40	
ν_1	0.02	0.07
E_2 [kJ/mol]	290.0	112.2
A_2 [s^{-1}]	6.0×10^{27}	8.2×10^{8}
n_2	2.65	0.97
ν_2	0.32	0.14
E_3 [kJ/mol]	149.4	
A_3 [s^{-1}]	1.3×10^{12}	1.0×10^{13}
n_3	1.20	1.12
ν_3	0.23	0.13
E_4 [kJ/mol]	175.4	
A_4 [s^{-1}]	6.0×10^{13}	2.2×10^{12}
n_4	2.10	1.25
ν_4	0.43	0.66
%dev_{TG}	0.6	1.0
%dev_{DTG}	2.1	1.6

The parameters of the first reaction step are invariant with the atmosphere apart from the higher amount of volatiles released in the presence of nitrogen (7 versus 2 wt%). Instead, the second step requires different parameters. In particular, the activation energy is rather high for the oxidative decomposition (290 versus 112 kJ/mol) which describes the release of significant amounts of volatiles (32 versus 14 wt%), corresponding to the peak rate. The third and fourth stage are well described by the same activation energies (149 and 175 kJ/mol) for the two reaction environments with the differences taken into account by variations on the remaining parameters. It is worth noticing that, for the oxidative decomposition, more than half of the polymer mass is lost during the second and third reaction step whereas, for thermal degradation, the largest amount of mass is lost during the fourth step (66 wt%) in correspondence of the maximum rate.

The differences in the decomposition kinetics (and devolatilization characteristics) originated by the reaction environment are

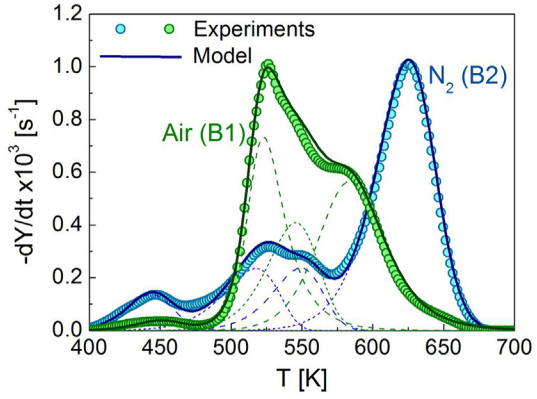

Fig. 2. Comparison between the measured (symbols) and the simulated (solid lined) mass fraction and rate of mass loss for PMMA with heating rate of 5 K/min in air (mechanism B1) and nitrogen (mechanism B2). Thin lines with various styles denote the predicted evolution of the rates of mass loss for the various reaction zones based on the kinetic parameters listed in Table 1.

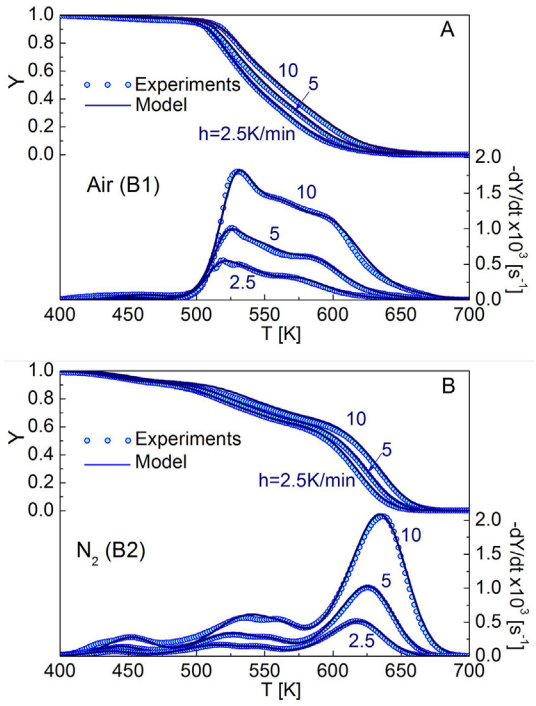

Fig.3A–B. Comparison between measured (symbols) and simulated (solid lines) thermogravimetric curves for the decomposition of PMMA at various heating rates, h, in air (mechanism B1, A) and nitrogen (mechanism B2, B) based on the kinetic parameters listed in Table 1.

so high that it is expected that, once incorporated in a transport model, quantitative predictions will be highly affected. In reality while, during steady burning, the presence of the flame hinders the diffusion of oxygen to solid surface, during the pre-ignition period the solid decomposition takes place in an oxidative environment [20]. Therefore, it is reasonable to consider the oxidative decomposition kinetics (model B1) for ascertaining the predictive capabilities of the transport model described below, though the physical transport of oxygen from the gas to the condensed phase is anyway neglected. On the other hand, for the post-ignition stage, not simulated in this study, the application of thermal decomposition kinetics (model B2) would be more appropriate. For comparison purposes, incorporation in the transport model of the thermal degradation kinetics B2 is also considered. Moreover, given its extensive use in previous literature, again for a sake of completeness, the usual single-step first-order thermal degradation reaction valid for low molecular weight PMMA, with the parameters estimated in Ref. [9] (activation energy 188 kJ/mol, pre-exponential factor of 1.32×10^{13} s^{-1}), is also given space.

Finally, the global reaction heat has also been evaluated (a sample mass 5.5 mg heated at 10 K/min up 800 K) leading to endothermic values of 880 J/g (air) or 875 J/g (nitrogen) which are practically coincident with the value of 870 J/g used in previous simulations [9,10].

4. Transport model

The one-dimension unsteady model for the thermal degradation of PMMA and PMMA/CNTs is that already presented [9,10] and makes use of the following assumptions:

- the polymer melting enthalpy is negligible,
- the specific heat and the thermal conductivity of both the composite and the parent polymer are temperature dependent,
- the polymer density is constant but the volume varies during the reaction,
- there is local thermal equilibrium among the phases,
- the thermal properties of the composite are modified by the dispersion of nanotubes,
- the effective thermal conductivity and the specific heat of the composite are modeled according to the geometric mean and the mixture rule, respectively,
- the composite thickness shrinks during the reaction process up to a maximum factor of 0.37 [37],
- upon reaction, the composite gives rise to a surface charred network consisting of tangled and stacked carbon nanotubes whose thermal conductivity is modeled by means of the Effective Medium Theory (EMT) equation,
- the thermal conductivity of the CNT bundles, formed upon reaction, is different from that of the CNTs in the virgin nanocomposite,
- the global thermal conductivity makes use of a parallel configuration for the nanocomposite and the charred superficial layer with contributions weighed on the basis of the polymer conversion, also including the radiative contribution,
- the convective transport of volatiles (validity of the ideal gas law) does not encounter any flow resistance and the pressure remains constant,
- the cone irradiance is absorbed in depth by the polymer (Beer law) and at the surface by the composite,
- the bottom surface of the sample is assumed to be adiabatic whereas the top surface is subject to convective heat transfer, with the global coefficient for the latter evaluated for a slab under natural convection [45] and corrected [46] to take into account the blowing effects associated with volatile product release,
- surface re-radiation is taken into account.

The solid phase model, after incorporations of the kinetic mechanisms B1 or B2 or the single step decomposition reaction as in Refs. [9,10], is coupled with the empirical ignition criteria based on the attainment of a critical surface temperature, T_c, or a critical volatile mass flux, m_c [47].

5. Results

In the first place, the model is applied for an extensive parametric analysis applying the multi-step thermo-oxidative kinetics (kinetics B1), aimed at clarifying the role of model assumptions (essentially the empirical ignition criteria) and parameters (intensity of the external heat flux, Q_0, and coefficient for the in-depth absorption of radiation for the neat polymer, β_s) on the predictions. A comparison is also proposed between the thermo-oxidative decomposition kinetics (kinetics B1) and the thermal decomposition kinetics for a high- or a low-molecular weight polymer (kinetics B2 or the single step global reaction). Then, the experimental validation of the model is carried out using the thermo-oxidative kinetics (kinetics B1). In addition to the decomposition kinetics and reaction heat discussed above, other input data include the in-depth radiation absorption coefficient ($1870 m^{-1}$ [48]), the polymer and nanocomposite emissivity (0.86 and 0.93 [49]), the carbon nanotube specific heat (3500 J/kgK [50]), the carbon nanotube density (1000 kg/m^3 [51]), the thermal conductivity of single carbon nanotubes and bundles on carbon nanotubes (3000 W/mK and 20 W/mK [52]) and the pore diameter (140 μm [9]). The sample density, 1100 kg/m^3, and thickness, 15 mm, and the carbon nanotube content of the composite, 1 wt%, are the same as those of the

cone calorimeter experiments. Computations have been made for a maximum grid size of 0.075 mm which provides grid-independent predictions and is almost one order of magnitude smaller that the attenuation distance (this grid size is also shorter for the attenuation distances of other literature absorption coefficients examined in the following).

5.1. Parametric analysis

Simulations of the mathematical model are made by varying the intensity of the cone irradiance in the range 15–100 kW/m^2 for slabs of the composite and the parent polymer (thermo-oxidative kinetics B1). The ignition times are predicted using the criteria based either on the critical surface temperature or the critical volatile mass flux. More specifically the upper and lower boundary of the ranges of values reported for PMMA [47] are considered: 553–593 K for the former and 1.82–4.5 g/m^{2}s for the latter, given that these parameters are dependent on the heating conditions and, most likely, on the specific properties of the polymer. Moreover, given the important role played by the in-depth radiation absorption coefficient for PMMA, the values reported in the literature for this parameter are also used for comparative simulations.

Fig. 4 reports the ignition times versus the cone irradiance, Q_0, for the composite and the parent polymer, as predicted with the two ignition criteria and the minimum and the maximum of the corresponding critical variables. In reality, the inverse of the square root of the ignition time is considered which, according to simplified analytical models [53], produces a straight line when the solid behaves as thermally thick (instead a straight line is produced by the inverse of the ignition time for a thermally thin sample [54]). A linear dependence is also shown by the predictions of this study unless very low irradiances (below 30 kW/m^2) are considered. Indeed, the thermal behavior, apart from the chemico-physical properties, depends on both the sample thickness and the heat flux intensity. As expected, in all cases, the ignition time becomes successively shorter as Q_0 is increased (obviously the lower boundary values of the ignition criteria result in a more rapid ignition) and the predicted value is significantly affected by the ignition criterion.

The PMMA ignition time is always longer when evaluated according to the T_c criterion, mainly at low heat fluxes. For the range of heat fluxes considered, it varies approximately in the ranges 955-11s (T_c = 553 K), 2390-19s (T_c = 593 K), 201-5s (m_c = 1.82 g/m^{2}s) and 563-6s (m_c = 4.5 g/m^{2}s), with reduction factors around 84 and 127 (T_c) or 39 and 93 (m_c) as Q_0 is increased. Thus the reduction factors on dependence of Q_0 are higher for the upper limits of the ignition criteria, especially for the critical surface temperature.

Again, for the entire range of external heating conditions, the composite ignition time is always longer for the T_c criterion except for very low irradiances (below 20 kW/m^2) and the upper limit of m_c, when ignition does not occur at all. It approximately varies in the ranges 444-4s (T_c = 553 K), 931-6s (T_c = 593 K), 225-2.5s (m_c = 1.82 g/m^{2}s) and 234-3s (m_c = 4.5 g/m^{2}s and Q_0 above 20 kW/m^2). The reduction factors on dependence of Q_0 are around 121 and 149 for the T_c criterion, which are higher than those of the parent polymer, a consequence of a direct link between surface temperature and external heat flux resulting from the absence of in-depth absorption of the radiation. Instead, for the m_c criterion, the reduction factors are 90 and 84 where the latter holds for Q_0 > 20 kW/m^2 (versus 39 and 23 for the parent polymer, given the same Q_0 range), as lower values do not give rise to ignition. It is understandable that, given relatively high m_c, degradation is not limited to a surface layer but also extends to a portion of the underlying sample. Thus the heat conduction mechanism is comparatively more important for the composite with respect to the polymer which also profits from in-depth absorption of radiation.

The thickness of the thermal layer, L_p, defined as the distance of the surface from the location where the temperature attains the value of 330 K, and reported versus the intensity of the cone irradiance in Fig. 5, confirms the above speculation. For the m_c criterion and both the polymer and the composite, L_p shows continuously decreasing values as Q_0 is increased. The same trend is also reproduced by the lower limit of T_c for the composite. For these conditions ignition occurs when the sample thickness is practically still coincident with the initial value (negligible sample consumption) though, as noticed above, the size of the degrading zone tends to become successively thicker as Q_0 is decreased. Moreover, for the T_c criterion, it may occur that significant sample consumption has already taken place at the ignition time, whose achievement is favored by the adiabatic sample bottom condition. This is the case for the pure polymer and Q_0 below 20 kW/m^2 (T_c = 553 K) or 35 kW/m^2 (T_c = 593 K) and the composite for Q_0 below 20 kW/m^2 (T_c = 593 K). Also, the thickness of the thermal layer (and the size of the reaction zone) at ignition is always larger for the polymer as long as surface regression is negligible.

The results, plotted in Figs. 4–5, suggest new insights in relation to the role of nanoparticles for the ignitability of composite materials. In fact, the action of carbon nanotubes appears to be affected by the ignition criterion, in the first place, and the cone irradiance. When the definition of ignition is based on the surface

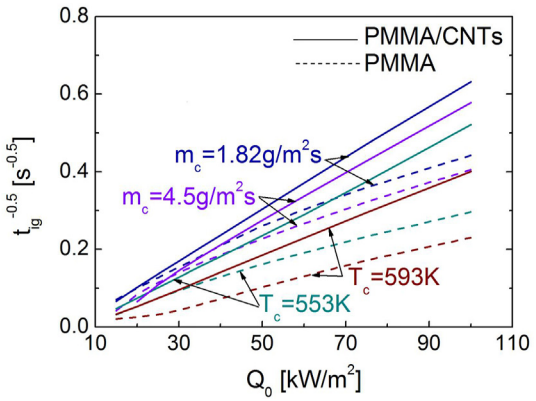

Fig. 4. Ignition times, t_{ig}, versus the cone irradiance, Q_0, for PMMA, and the PMMA/CNTs composite evaluated according to the critical surface temperature, T_c, or the critical mass flux, m_c, criterion.

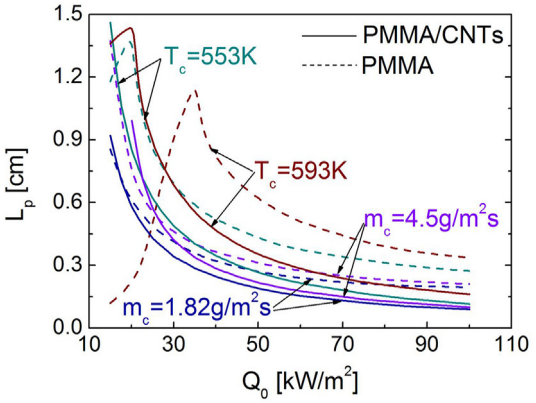

Fig. 5. Thickness of the thermal layer, at the ignition time as evaluated for PMMA and the PMMA/CNTs composite according to the critical surface temperature and mass flux criteria, versus the external heat flux.

temperature, nanocomposite always ignites first. Instead, the composite requires longer ignition times, based on the volatile product rates, for low external heat fluxes (up to 17.5 and 27.5 kW/m^2 for the lower and upper value of m_c) and then ignition becomes again more favored. These findings can be explained taking into account that, for very mild external heating conditions, the ignition times are attained at times so long that, following the thermo-oxidative degradation of the composite, a surface charred barrier is formed performing the usual flame retardancy action. However, as the external heating conditions become more severe, the mechanism of surface absorption of the thermal radiation locally enhances the decomposition rate leading to shorter ignition times with respect to the in-depth absorbing polymer.

In reality, owing to the central role of sample heating, which also directly influences the degradation rate, the in-depth radiation absorption coefficient can also, in its turn, be determinant for the ignition performances of the composite versus the parent polymer, thus this aspect is further examined. A rather wide range of coefficients for the in-depth absorption of radiation, β_s, for PMMA is reported by previous literature, in addition to the value selected here (1870m^{-1} [48]): 10000 m^{-1} [55,56], 2700 m^{-1} [34], 150 m^{-1} [57]. To clarify this issue, the ignition times are again evaluated from simulations carried out by varying the external heat flux and β_s according to the values listed above (thermo-oxidative kinetics B1). Figs. 6–8 report the ignition times versus Q_0, as predicted for the composite and the PMMA samples with the above range of β_s values using the two criteria. The qualitative trend of the predicted ignition times versus Q_0 is the same as already discussed for the reference value of β_s. More specifically, according to the critical surface temperature criterion, the composite always ignites first while an inversion (in some case with no ignition at all) is observed for low external heat fluxes (values dependent on β_s) when the critical mass flux criterion is applied. From the quantitative point of view, the PMMA ignition times tend to approach those of the composite as β_s is progressively increased, that is, as the in-depth dispersion of the cone heat flux becomes less effective though ignition, defined according to the critical surface temperature, is always facilitated for the composite. In fact the corresponding temporal profiles of the surface temperature (Fig. 9A–B) confirm that the heating rate of the composite surface is always faster than that of the parent polymer independently from β_s and Q_0. The differences obviously tend to reduce as β_s is increased.

The temporal profiles of the mass flux for the polymer (various β_s) and the composite, compared with the limit values of the ignition criterion in Fig. 10A–C, clearly show the reduced

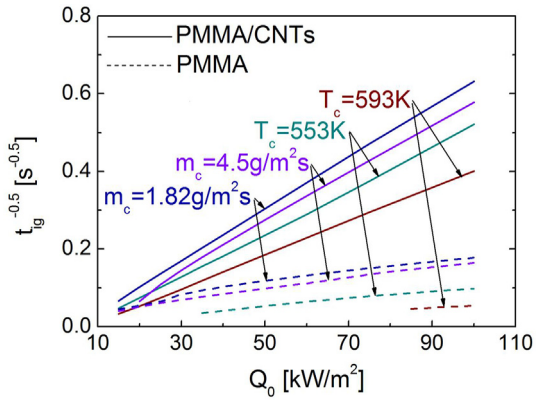

Fig. 6. Ignition times, t_{ig}, versus the cone irradiance, Q0, for PMMA ($\beta_s = 150$ m^{-1}), and the PMMA/CNTs composite evaluated according to the critical surface temperature, T_c, or the critical mass flux, m_c, criterion.

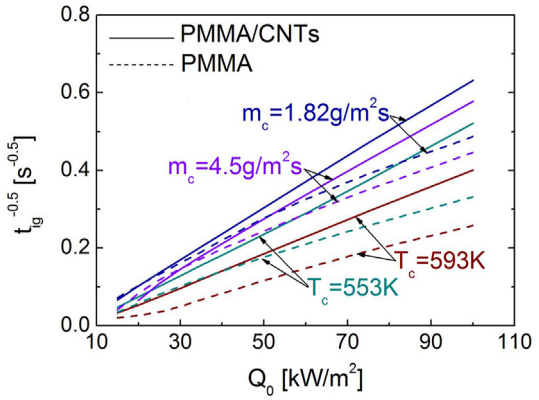

Fig. 7. Ignition times, t_{ig}, versus the cone irradiance, Q0, for PMMA ($\beta_s = 2700$ m^{-1}), and the PMMA/CNTs composite evaluated according to the critical surface temperature, T_c, or the critical mass flux, m_c, criterion.

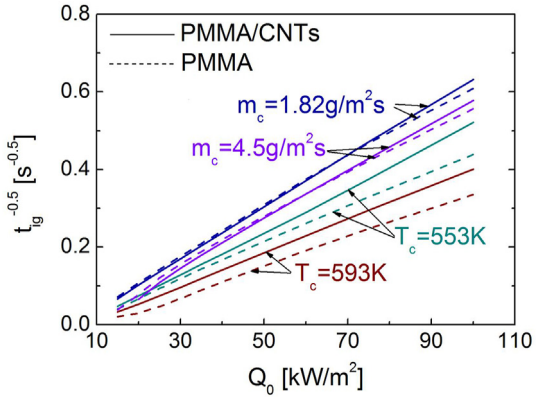

Fig. 8. Ignition times, t_{ig}, versus the cone irradiance, Q_0, for PMMA ($\beta_s = 10000$ m^{-1}), and the PMMA/CNTs composite evaluated according to the critical surface temperature, T_c, or the critical mass flux, m_c, criterion.

ignitability of the latter, for low external heat fluxes over the higher value range of β_s. More specifically the increase in the ignition delay time of the composite is preserved for successively higher Q_0 as β_s assumes successively higher values, that is, as the ability of the pure polymer to hold heat at the surface is enhanced. For the ranges of β_s examined and the lower m_c limit, the Q_0 value for the inversion increases from about 15 to 70 kW/m^2. For the upper limit of m_c, a highly in-depth absorbing polymer ($\beta_s = 150$ m^{-1}) is always more resistant to ignition unless the external heat flux is so low (<20 kW/m^2) that the composite does not ignite. For higher β_s, the composite always shows longer ignition times for Q_0 below 60 kW/m^2.

5.2. Influence of the thermal and thermo-oxidative kinetics

In order to evaluate the influence of the multi-step kinetic mechanism B1 (air) or B2 (nitrogen), simulations have been made for the polymer and the composite varying the intensity of the external heat flux in the range 15–100 kW/m^2. To facilitate the comparison, only the average values of the critical parameters for ignition are considered with reference to the ranges used above, i.e. 570 K for the surface temperature and 3 g/m^{2}s for the mass flux. As shown in Fig. 11A–B, the role played by the reaction atmosphere depends on the ignition criterion, the external heat flux intensity and the properties of the sample (either polymer or composite). For PMMA, when the critical surface temperature criterion is applied,

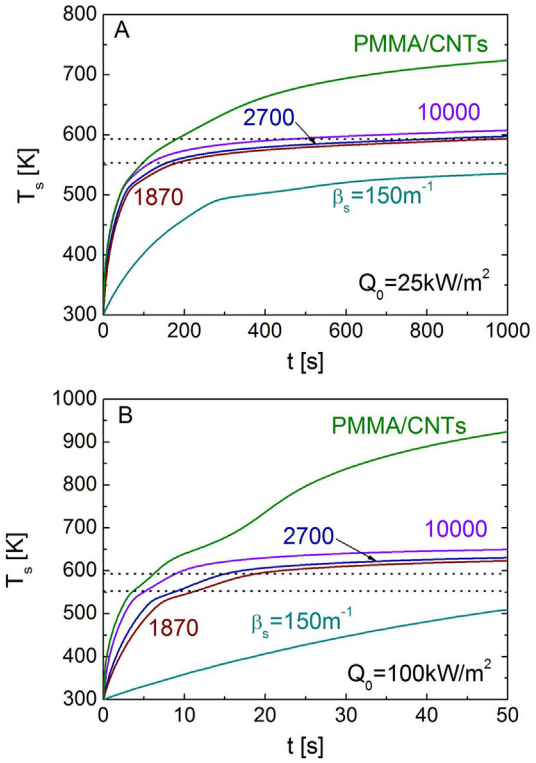

Fig. 9A–B. Surface temperature versus time for PMMA and several β_s values and PMMA/CNTs composite for external heat fluxes of 25 kW/m^2 (A) and 100 kW/m^2 (B) (the range of critical surface temperatures, T_c, for ignition is indicated by the dotted lines).

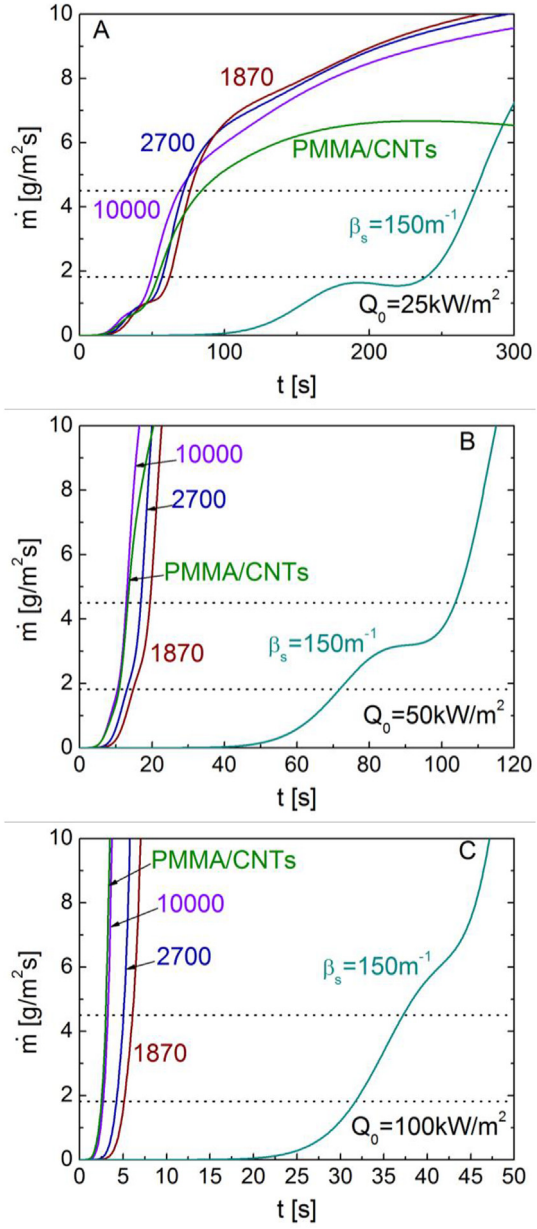

Fig. 10A–C. Volatile mass flux versus time for PMMA and several β_s values and PMMA/CNTs composite for external heat fluxes of 25 kW/m^2 (A), 50 kW/m^2 (B) and 100 kW/m^2 (C) (the range of critical mass fluxes for ignition, m_c, is indicated by the dotted lines).

the ignition delay time is always shorter in nitrogen though the differences tend to reduce as Q_0 is increased (the ratio between the two times decreases from about 2.4 to 1.3 for the range of heat fluxes examined). The temporal profiles of the surface temperature (Fig. 12A–B) confirm that, for the range of critical values, the heating rate is always faster in nitrogen. This finding is attributable to the reduced convective cooling [58,59] resulting from the attainment of significant rates of volatile release at higher temperatures compared with the thermo-oxidative conditions (see Fig. 1). The same trend is also observed for the PMMA/CNTs samples though the quantitative differences are highly reduced and the dependence on the external heat flux is significantly weaker (ratios around 1.1). It can be hypothesized that, for the composite, the surface heating characteristics essentially depends on the formation of a charred layer and its properties which are scarcely affected by the reaction environment. Moreover, based on the T_c criterion, for both air and nitrogen atmosphere, the composite always ignites first than the pure polymer.

The ignition times for pure PMMA, evaluated according to the critical mass flux, present a more complex dependence on the reaction atmosphere, with respect to the critical surface temperature criterion, as they are significantly affected by the multi-step features of the decomposition kinetics. More specifically, compared with the inert atmosphere, the predicted ignition times in air for the polymer are shorter for very low heat fluxes (up to about 22 kW/m^2) and then become longer (the maximum difference, corresponding to a factor of about 1.5, is attained for intermediate heat fluxes around 25–40 kW/m^2). As shown by the temporal profiles of the mass flux, reported in Fig. 13A–B, the performance of the polymer in air or nitrogen are significantly dependent on the relative importance of the first, low-temperature step of the thermal decomposition kinetics B2 with respect to the second much faster step of the thermo-oxidative kinetics B1 which, apart from the m_c value, is affected by the intensity of the external heat flux. As a consequence of the change in the dominant step in the mechanism B2, the slope for the predicted ignition times versus Q_0 exhibit a sharp variation. Similar to the behavior observed for the polymer, the predicted ignition times for the composite are shorter in air at low heat fluxes (up to about 30 kW/m^2) and then become longer (approximately by a factor around 1.3) as a consequence of the changes in the relative importance of the low-temperature steps in the mechanisms B1 and B2. It should also be noticed that, independently from the reaction atmosphere, when the critical mass flux criterion in employed, the ignition time of the nanocomposite is longer than that of the parent polymer at low

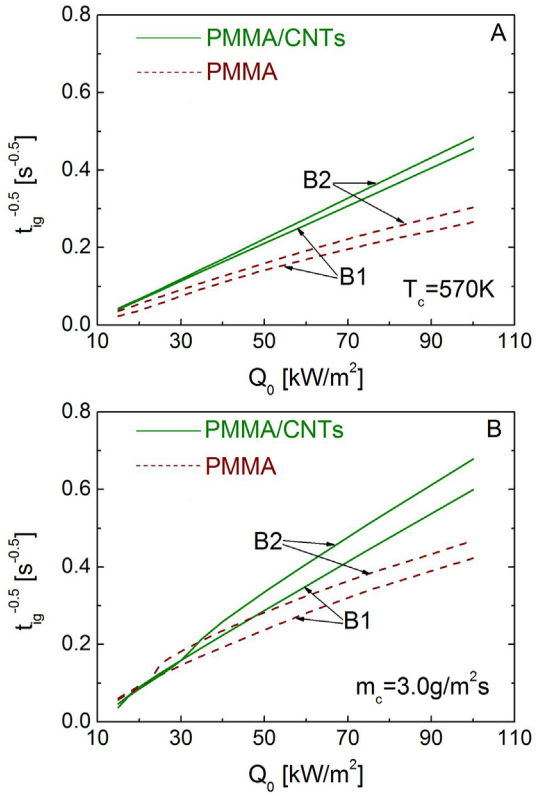

Fig. 11A–B. Ignition times, t_{ig}, versus the cone irradiance, Q_0, for PMMA, and the PMMA/CNTs composite evaluated according to the critical surface temperature ($T_c = 570$ K, A) or the critical mass flux ($m_c = 3$ g/m^{2}s, B) criterion using the mechanism B1 (air) or B2 (nitrogen).

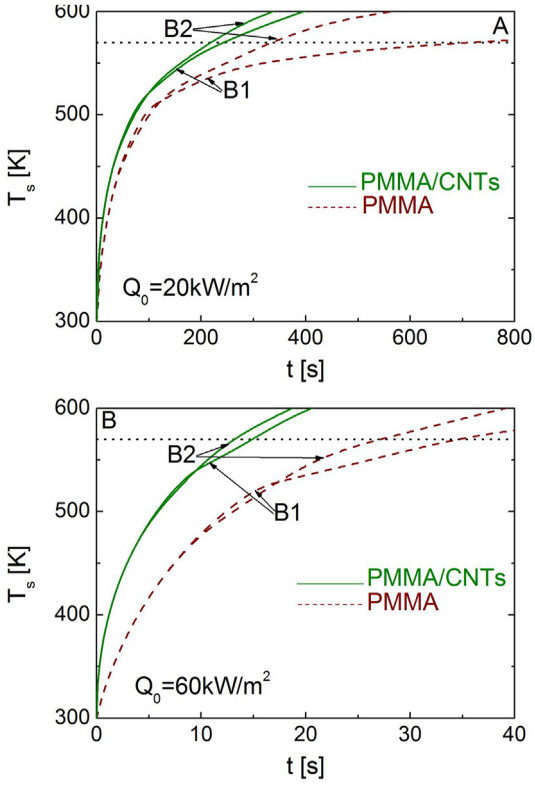

Fig. 12A–B. Surface temperature versus time for PMMA and PMMA/CNTs composite for external heat fluxes of 20 kW/m^2 (A) and 60 kW/m^2 (B) (the T_c value is indicated by a dotted line), as simulated with the mechanism B1 (air) or B2 (nitrogen).

heat fluxes (up to about 20 kW/m^2 in air and 32 kW/m^2 in nitrogen).

Significant differences are also observed between the ignition times predicted by the kinetics B2 and the single step decomposition reaction of PMMA (influences of the polymerization degree for conditions of thermal decomposition). For the both the polymer and the composite, the single-step mechanism gives rise to longer times when the critical mass flux is used whereas the contrary occurs for the critical surface temperature criterion (not shown in figures). The occurrence of the decomposition process at higher temperatures justifies the former result. On the other hand, this features is also associated with a faster rate of surface heating consequent to reduced convective cooling [58,59], thus explaining the shorter ignition times based on the T_c criterion. From the quantitative point of view, for increasing values of Q_0, the ignition times for the single-step reaction are longer than those of the four-step mechanism B2 by factors of about 4–3 and shorter by factors of about 1.6–1.2 for the two criteria (critical mass flux and surface temperature, respectively).

5.3. Experimental validation

As already pointed out, the ignition times have been measured in a cone calorimeter for PMMA and PMMA/CNTs samples (thickness 15 mm and CNTs content 1 wt%) that behave according to multi-step decomposition kinetics, resulting from a high polymerization degree. Moreover, from the quantitative point of view, the kinetic parameters are affected by the reaction environment. In addition to the selection of the kinetics determined for oxidative conditions, the comparison between predictions and measurements also requires a motivated choice of the of the ignition criterion, given its significant role from the quantitative point of view. It is indubitable that the ignition temperature has been widely applied to correlate piloted ignition times under well defined conditions though it is an empirical parameter [60]. On the contrary, the critical mass flux criterion is more physically sound and has been reported to give the best predictions [61]. Therefore this criterion is used for a comparison between prediction and experiments using the average value (0.3 g/m^{2}s) of the range provided in Ref. [47]. As shown in Fig. 14, both model and measurements indicate that the nanocomposite is more resistant to ignition at low heat fluxes (values approximately below 25 kW/m^2), a feature that is completely missed by the ignition temperature criterion. On the whole, taking into account the simplifications introduced in the mathematical description of the problem, the agreement between predictions and measurements is good. Though the cone calorimeter data are usually collected for intermediate values of the irradiation (typically 50 kW/m^2), another study [62] also reports the same trend observed here. Indeed, the ignition times are actually longer than those of the parent polymer when the intensity of the external heat flux is very low followed by an inversion when the thermal severity of the heating process is increased. On the other hand, it is also known that the magnitude of the fire retardancy effects of nanocomposites depends on the external heating conditions [13].

6. Conclusions

A comprehensive solid-phase model of PMMA and PMMA/CNTs decomposition has been coupled with empirical criteria to study the ignition of thick samples in a cone calorimeter. As expected, the

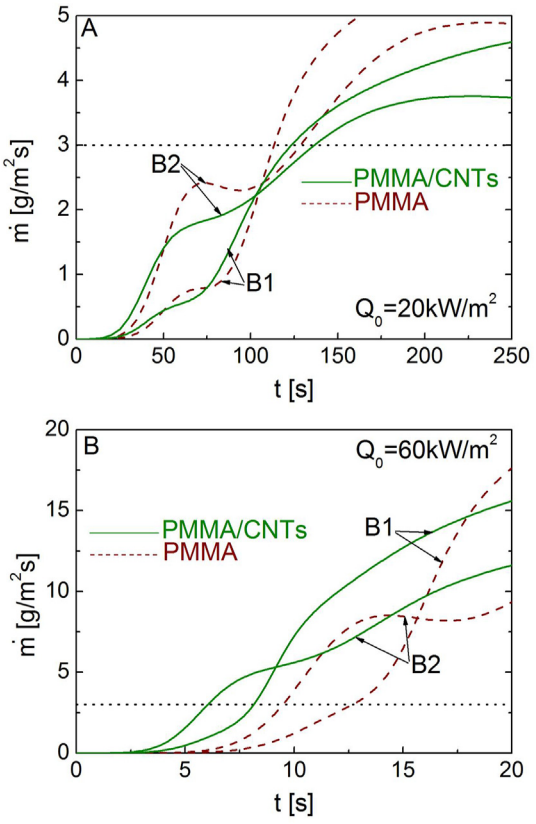

Fig. 13A–B. Volatile mass flux versus time for PMMA and PMMA/CNTs composite for external heat fluxes of 20 kW/m^2 (A) and 60 kW/m^2 (B) (the m_c value is indicated by a dotted line), as simulated with the mechanism B1 (air) or B2 (nitrogen).

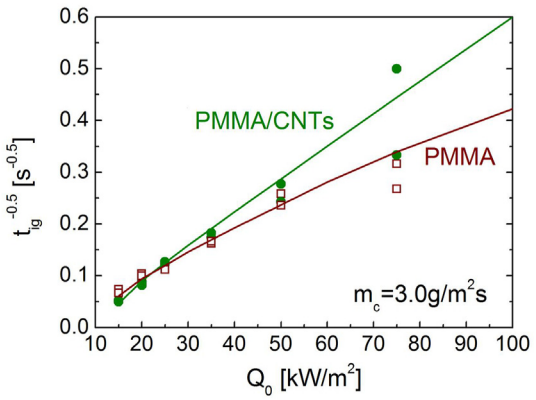

Fig. 14. Predictions, as evaluated for a critical mass flux $m_c = 3$ g/m^{2}s (solid lines), and measurements (symbols) of the ignition time, t_{ig}, in a cone calorimeter for PMMA and PMMA/CNTs versus the intensity of the external heat flux, Q_0.

predicted ignition times decrease as the radiation intensity is increased with values dependent on the ignition criterion and the polymer properties. However the radiation absorption modality (superficial for the nanocomposite and volumetric for the parent polymer) determines the improvement or deterioration in the ignitability of the composite versus the pure polymer.

In quantitative agreement with the measurements, when compared with the pure polymer, the composite exhibits longer ignition times at very low heat fluxes whereas the opposite is observed at high values. In fact, for mild heating, a charred surface layer is formed, owing to the presence of carbon nanotubes, which delays the attainment of a critical volatile mass flux. Instead, for severe heating, the faster degradation of the surface causes volatile release rates higher than those of the in-depth heated raw polymer.

The selection of the ignition criterion (critical mass flux or surface temperature) as well as the actual critical values highly affect the predicted performances of the nanocomposite versus the polymer. Apart from the decomposition kinetics that, as shown in this study, depends on the specific properties of the polymer, the radiation absorption properties of the samples are also crucial in relation to ignitability.

Acknowledgements

This work is part of the activities carried out in the framework of the project COCET “Comportamento di Materiali Compositi in Condizioni Estreme: Alta Temperatura” (PON02_00029_3206086/F1), coordinated by IMAST and funded by the Italian Ministry of Instruction, University and Research (MIUR), the partial support of which is gratefully acknowledged.

References

[1] F. Laoutid, L. Bonnaud, M. Alexandre, J.-M. Lopez-Cuesta, P. Dubois, New prospects in flame retardant polymer materials: from fundamentals to nanocomposites, Mat. Sci. Eng. R. 63 (2009) 100–125.
[2] P. Kiliaris, C.D. Papaspyrides, Polymer/layered silicate (clay) nanocomposites: an overview of flame retardancy, Prog. Polym. Sci. 35 (2010) 902–958.
[3] A.B. Morgan, J.W. Gilman, An overview of flame retardancy of polymeric materials: application, technology, and future directions, Fire Mater 37 (2013) 259–279.
[4] J. Alongi, Z. Han, S. Bourbigot, Intumescence: tradition versus novelty. A comprehensive review, Prog. Polym. Sci. 51 (2015) 28–73.
[5] C. Di Blasi, C. Branca, A mathematical model for the non-steady decomposition of intumescent coatings, AIChE J. 47 (2001) 2359–2370.
[6] C. Di Blasi, Modeling the effects of high radiative heat fluxes on intumescent material decomposition, J. Anal. Appl. Pyrol 71 (2004) 721–737.
[7] J. Zhang, M.A. Delichatsios, S. Bourbigot, Experimental and numerical study of the effects of nanoparticles on pyrolysis of polyamide 6 (PA6) nanocomposite in the cone calorimeter, Combust. Flame 156 (2009) 2056–2062.
[8] S.S. Rahatekar, M. Zammarano, S. Matko, K.K. Koziol, A.H. Windle, M. Nyden, T. Kashiwagi, G.W. Gilman, Effect of carbon nanotubes and montmorillonite on the flammability of epoxy nanocomposites, Polym. Degrad. Stab. 95 (2010) 870–879.
[9] C. Di Blasi, A. Galgano, C. Branca, Modeling the thermal degradation of poly(methyl methacrylate)/carbon nanotube nanocomposites, Polym. Degrad. Stab. 98 (2013) 266–275.
[10] C. Di Blasi, A. Galgano, Influences of properties and heating characteristics on the thermal decomposition of polymer/carbon nanotube nanocomposites, Fire Saf. J. 59 (2013) 166–177.
[11] B. Schartel, T.B. Hull, Development of fire-retarded materials. Interpretation of cone calorimeter data, Fire Mater 31 (2007) 327–354.
[12] B. Schartel, M. Bartholmai, U. Knoll, Some comments on the main fire retardance mechanisms in polymer nanocomposites, Polym. Adv. Technol. 17 (2006) 772–777.
[13] B. Schartel, U. Knoll, A. Hartwig, D. Putz, Phosphonium-modified layered silicate epoxy resins nanocomposites and their combinations with ATH and organo-phosphorus fire retardants, Polym. Adv. Technol. 17 (2006) 281–293.
[14] J. Zhu, F.M. Uhl, A.B. Morgan, C.A. Wilkie, Studies on the mechanism by which the formation of nanocomposites enhances thermal stability, Chem. Mater 13 (2001) 4649–4654.
[15] H. Mauroy, T.S. Plivelic, E.L. Hansen, J.O. Fossum, G. Helgesen, K.D. Knudsen, Effect of clay surface charge on the emerging properties of polystyrene organoclay nanocomposites, J. Phys. Chem. C 117 (2013) 19656–19663.
[16] S. Majoni, Thermal and flammability study of polystyrene composites containing magnesium aluminum layered double hydroxide (MgAlC16 LDH), and an organophosphate, J. Therm. Anal. Calorim. 120 (2015) 1435–1443.
[17] B. Dittrich, K.A. Wartig, D. Hofmann, R. Mülhaupt, B. Schartel, Flame retardancy through carbon nanomaterials: Carbon black, multiwall nanotubes, expanded graphite, multi-layer graphene and graphene in polypropylene, Polym. Degrad. Stab. 98 (2013) 1495–1505.
[18] B. Schartel, A. Weiss, F. Mohr, M. Kleemeier, A. Hartwig, U. Braun, Flame retarded epoxy resins by adding layered silicate in combination with the conventional protection-layer-building flame retardants melamine borate and ammonium polyphosphate, J. Appl. Polym. Sci. 118 (2010) 1134–1143.
[19] T. Kashiwagi, E. Grulke, J. Hilding, K. Groth, R. Harris, K. Butler, J. Shields, S. Kharchenko, J. Douglas, Thermal and flammability properties of polypropylene/carbon nanotube nanocomposites, Polymer 45 (2004) 4227–4239.

[20] A. Fina, G. Camino, Ignition mechanisms in polymers and polymer nanocomposites, Polym. Adv. Technol. 22 (2011) 1147–1155.
[21] H. Vahabi, M.A. Batistella, B. Otazaghine, C. Longuet, L. Ferry, R. Sonnier, J.-M. Lopez-Cuesta, Influence of a treated kaolinite on the thermal degradation and flame retardancy of poly(methyl methacrylate), Appl. Clay Sci. 70 (2012) 58–66.
[22] H. Qin, Q. Su, S. Zhang, B. Zhao, M. Yang, Thermal stability and flammability of polyamide 66/montmorillonite nanocomposites, Polymer 44 (2003) 7533–7538.
[23] S. Bourbigot, F. Samyn, T. Turf, S. Duquesne, Nanomorphology and reaction to fire of polyurethane and polyamide nanocomposites containing flame retardants, Polym. Degrad. Stab. 95 (2010) 320–326.
[24] M. Lewin, Flame retarding polymer nanocomposites: Synergism, cooperation, antagonism, Polym. Degrad. Stab. 96 (2011) 256–269.
[25] M.R. Schütz, H. Kalo, T. Lunkenbein, J. Breu, C.A. Wilkie, Intumescent-like behavior of polystyrene synthetic clay nanocomposites, Polymer 52 (2011) 3288–3294.
[26] S. Peeterbroeck, F. Laoutid, B. Swoboda, J.M. Lopez-Cuesta, N. Moreau, J.B. Nagy, M. Alexandre, P. Dubois, How Carbon Nanotube Crushing can Improve Flame Retardant Behaviour in Polymer Nanocomposites? Macromol. Rapid Commun. 28 (2007) 260–264.
[27] B.N. Jang, C.A. Wilkie, The thermal degradation of polystyrene nanocomposite, Polymer 46 (2005) 2933–2942.
[28] P. Wei, S. Bocchini, G. Camino, Nanocomposites combustion peculiarities. A case history: Polylactide-clays, Eur.Polym. J. 49 (2013) 932–939.
[29] H. Qin, S. Zhang, C. Zhao, G. Hu, M. Yang, Flame retardant mechanism of polymer/clay nanocomposites based on polypropylene, Polymer 46 (2005) 8386–8395.
[30] R.E. Gorga, R.E. Cohen, Toughness enhancements in poly(methyl methacrylate) by addition of oriented multiwall carbon nanotubes, J. Polym. Sci. Part B Polym. Phys. 42 (2004) 2690–2702.
[31] D. Hopkins, Predicting the Ignition Time and Burning Rate of Thermoplastics in the Cone Calorimeter, Master Thesis, University of Maryland, 1995. NIST-GCR-95–677.
[32] B.J. Holland, J.N. Hay, The effect of polymerisation conditions on the kinetics and mechanisms of thermal degradation of PMMA, Polym. Degrad, Stab 77 (2002) 435–439.
[33] T. Hirata, T. Kashiwagi, J.E. Brown, Thermal and oxidative degradation of poly(methylmethacrylate): weight loss, Macromolecules 18 (1985) 1410–1418.
[34] S.I. Stoliarov, S. Crowley, R.E. Lyon, G.T. Linteris, Prediction of the burning rates of non-charring polymers, Combust. Flame 156 (2009) 1068–1083.
[35] M. Ferriol, A. Gentilhomme, M. Cochez, N. Oget, J.L. Mieloszynski, Thermal degradation of poly(methyl methacrylate) (PMMA): modelling of DTG and TG curves, Polym. Degrad. Stab. 79 (2003) 271–281.
[36] L.E. Manring, Thermal degradation of poly(methyl methacrylate), 2. Vinyl-terminated Polym. Macromol. 22 (1989) 2673–2677.
[37] T. Kashiwagi, F. Du, K.I. Winey, K.M. Groth, J.R. Shields, S.P. Bellayer, H. Kim, J.F. Douglas, Flammability properties of polymer nanocomposites with single-walled carbon nanotubes: effects of nanotube dispersion and concentration, Polymer 46 (2005) 471–481.
[38] B.H. Cipriano, T. Kashiwagi, S.R. Raghavan, Y. Yang, E.A. Grulke, K. Yamamoto, J.R. Shields, J.F. Douglas, Effects of aspect ratio of MWNT on the flammability properties of polymer nanocomposites, Polymer 48 (2007) 6086–6096.
[39] C. Branca, C. Di Blasi, H. Horacek, Analysis of the combustion kinetics and the thermal behaviour of an intumescent system, Ind. Eng. Chem. Res. 41 (2002) 2104–2114.
[40] C. Branca, C. Di Blasi, A. Casu, V. Morone, C. Costa, Reaction kinetics and morphological changes of a rigid polyurethane foam during combustion, Thermochim. Acta 399 (2003) 127–137.
[41] C. Branca, C. Di Blasi, R. Elefante, Devolatilization and heterogeneous combustion of wood fast pyrolysis oils, Ind. Eng. Chem. Res. 44 (2005) 799–810.
[42] C. Branca, C. Di Blasi, A. Galgano, E. Milella, Thermal and kinetic characterization of a toughened epoxy resin reinforced with carbon fibres, Thermochim. Acta 517 (2011) 53–62.
[43] C. Branca, C. Di Blasi, A unified mechanism of the combustion reactions of lignocellulosic fuels. Thermochim, Acta 565 (2013) 58–64.
[44] C. Branca, C. Di Blasi, Char structure and combustion kinetics of a phenolic-impregnated honeycomb material, Ind. Eng. Chem. Res. 52 (2013) 14574–14582.
[45] R.H. Perry, D.W. Green, J.O. Maloney (Eds.), Perry's Chemical Engineers' Handbook, sixth ed., McGraw-Hill, New York, 1984.
[46] T.K. Sherwood, R.L. Pigford, C.R. Wilke, Mass Transfer, McGraw-Hill, New York, 1975.
[47] R.E. Lyon, J.G. Quintiere, Criteria for piloted ignition of combustible solids, Combust. Flame 151 (2007) 551–559.
[48] G. Linteris, M. Zammarano, B. Wilthan, L. Hanssen, Absorption and reflection of infrared radiation by polymers in fire-like environments, Fire Mater 36 (2012) 537–553.
[49] www.infraredheaters.com/pdfs/radiant.pdf.
[50] N.R. Pradhan, G.S. Iannacchione, Thermal properties and glass transition in PMMA + SWCNT composites, J. Phys. D. Appl. Phys. 43 (2010) 1–9, 305403.
[51] S. Daniel, T.P. Rao, K.S. Rao, S.U. Rani, G.R.K. Naidu, H. Y.Lee, et al., A review of DNA functionalized/grafted carbon nanotubes and their characterization, Sens. Actuat B-Chem 122 (2007) 672–682.
[52] D.J. Yang, Q. Zhang, G. Chen, S.F. Yoon, J. Ahn, S.G. Wang, et al., Thermal conductivity of multiwalled carbon nanotubes, Phys. Rev. B Condens Matter 66 (2002) 1–6, 165440.
[53] J. Torero, Flaming Ignition of Solid Fuels, SFPE Handbook of Fire Protection Engineering, Chp. 21, Springer New York, 2016, pp. 633–661.
[54] M.A. Delichatsios, Piloted ignition times, critical heat fluxes and mass loss rates at reduced oxygen atmospheres, Fire Saf. J. l40 (2005) 197–212.
[55] T. Kashiwagi, A radiative ignition model of a solid fuel, Combust. Sci. Technol. 8 (1974) 225–236.
[56] C. Di Blasi, S. Crescitelli, G. Russo, G. Cinque, Numerical model of ignition processes of polymeric materials including gas phase absorption of radiation, Combust. Flame 83 (1991) 333–344.
[57] Y. Nakamura, T. Kashiwagi, Effects of sample orientation on nonpiloted ignition of thin poly(methyl methacrylate) sheet by a laser. 1. Theoretical prediction, Combust. Flame 141 (2005) 149–169.
[58] C. Di Blasi, Influences of model assumptions on the predictions of cellulose pyrolysis in the heat transfer controlled regime, Fuel 75 (1996) 58–66.
[59] C. Di Blasi, Modelling intra- and extra-particle processes of wood fast pyrolysis, AIChE J. 48 (2002) 2386–2397.
[60] D. Rich, C. Lautenberger, J.L. Torero, J.G. Quintiere, C. Fernandez-Pello, Mass flux of combustible solids at piloted ignition, Proc. Combust. Inst. 31 (2007) 2653–2660.
[61] I. Vermesi, N. Roenner, P. Pironi, R.M. Hadden, G. Rein, Pyrolysis and ignition of a polymer by transient irradiation, Combust. Flame 163 (2016) 31–41.
[62] A. Fina, F. Cuttica, G. Camino, Ignition of polypropylene/montmorillonite nanocomposites, Polym. Degrad. Stabil. 97 (2012) 2619–2626.